Optimum Design of Space Storable Gas/Liquid Coaxial Injectors

R. J. BURICK*
Rocketdyne/Rockwell International, Canoga Park, Calif.

Results from an experimental program are presented whose objective was to establish performance and chamber compatibility design criteria for circular coaxial injector concepts for application with the space storable gas/liquid propellant combination FLOX (82.6% F_2, 17.4% O_2)/CH_4(g) at high pressure. The primary goal of the program was to obtain high characteristic velocity efficiency ($\eta_{c^*} \geq 99\%$) in conjunction with acceptable injector/chamber compatilibity. Subscale (single-element) cold-flow and hot-fire experiments were employed to establish design criteria for a 3000 lbf (sea level) engine operating at 500 psia. The subscale experiments characterized both high performance "core" elements and "peripheral" elements with enhanced injector/chamber compatibility. The full-scale injector which evolved from the study demonstrated a performance level of 99% of the theoretical shifting characteristic exhaust velocity with low chamber heat flux levels. At the design condition ($P_c = 500$ psia), measured heat flux levels were approximately 2 to 3 Btu/in.^{2}-sec in the graphite cylindrical chamber; the heat flux levels were predicted by initial program efforts with subscale, low-cost, single-element hardware. Full-scale injector durability was demonstrated during a 44-sec firing; additionally, dynamic stability was demonstrated by a 15-msec recovery to a 1100 psi chamber overpressure.

Introduction

THE work reported herein is the result of a program of analysis, design, and experiments to evaluate the circular coaxial injector concept for high-performance space-storable rocket engine applications. Coaxial injector concepts consist of a central liquid (usually oxidizer) jet which is surrounded by an annulus of high-velocity gas (usually fuel). In this study, both the geometric and operating variables of the coaxial element were systematically investigated to determine their effect on performance and chamber wall heat flux characteristics.

To establish design criteria for a full-scale injector, cold-flow and hot-fire experiments were conducted with single-element models. Pressurized cold-flow experiments (mixing and atomization) were employed to investigate geometric and operating variables with the intent of maximizing element performance and assessing potential chamber wall heat flux characteristics. The use of cold-flow techniques permitted detailed diagnostic evaluation of the flowfields as well as delineation of the controlling variables; additionally, the use of single-element models provided substantial program cost savings.

Previous investigations have employed an analogous approach to establish design criteria for liquid/liquid systems.[1,2] Thus, this effort represents a logical extension of similar cold-flow/hot-fire techniques to establish design criteria for high-performance gas/liquid systems.

To investigate chamber wall heat transfer characteristics of candidate elements, cold-flow mixing experiments were conducted to determine wall zone mass and mixture ratio distributions. Previous programs have shown that wall zone mass and mixture ratio distributions are the controlling variables for chamber wall heat flux levels.[1]

Presented as Paper 72-1076 at the AIAA/SAE 8th Joint Propulsion Specialist Conference, New Orleans, La., November 29–December 1, 1972; submitted December 6, 1972; revision received June 8, 1973. Sponsored by NASA Lewis Research Center under Contract NAS3-12051.

Index categories: Liquid Rocket Engines; Combustion in Heterogeneous Media, Multiphase Flows.

* Member of the Technical Staff, Advanced Programs. Member AIAA.

Experimental Studies

Element Selection and Operating Conditions

The nominal thrust level of the circular coaxial element that was selected for characterization was 70-lbf FLOX/CH_4(g) at optimum sea level expansion. The nominal design values for the hot-fire operating conditions were as follows: $P_c = 500$ psia; oxidizer/fuel mixture ratio = 5.25; fuel temperature = 530°R; FLOX density = 89 lbm/ft^3.

A schematic of the core element which was characterized is shown in Fig. 1. In the cold-flow investigation, the primary design variables which were studied were the liquid oxidizer orifice size, the gaseous fuel orifice size (or annulus), and the amount of recess of the oxidizer post. The operating variables which were independently investigated were the injected gas velocity, injected liquid velocity, injected mass flow ratios ($\dot{w}_{liq}/\dot{w}_{gas}$), and the gas-phase density.

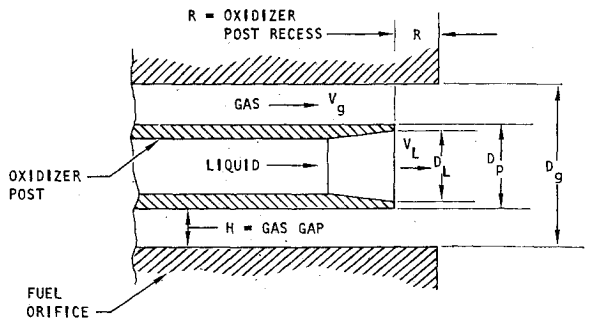

CORE ELEMENT CONFIGURATIONS (NOMINAL DIMENSIONS)			
NO.	D_L, IN.	D_P, IN.	D_g, IN.
1	0.136	0.146	0.182
2	0.108	0.122	0.166
3	0.070	0.080	0.136

Fig. 1 Core element configuration.

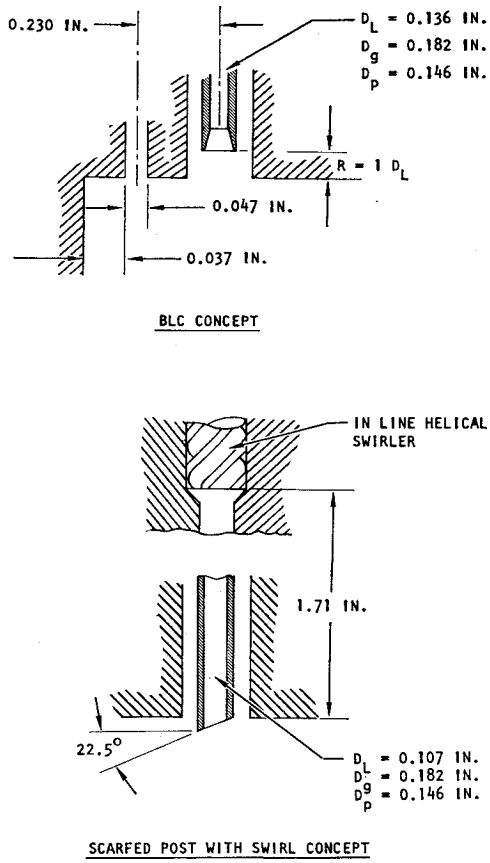

Fig. 2 Peripheral element configurations.

Two peripheral element configurations were characterized. A baseline configuration was selected which consisted of a core-type element with an adjacent boundary-layer coolant (BLC) orifice. The second peripheral element configuration consisted of a scarfed post with oxidizer jet swirl. Schematics of the two elements along with their respective dimensions are shown in Fig. 2. Note that the gas annulus gaps were equal so that each configuration operated with equivalent gas injection velocities. In the scarfed post configuration, an in-line helical swirler was employed to swirl the liquid oxidizer jet.

Core Element Cold-Flow Results

Parametric mixing and atomization experiments were conducted to determine the independent effects of gas velocity, liquid velocity, throttling (gas density), element mixture ratio, and oxidizer post recess. The results of those studies are summarized in Ref. 3, and detailed information can be found in Ref. 4.

Peripheral Element Cold-Flow Results

Extensive atomization experiments were not conducted with the peripheral elements because limited experiments showed that resulting drop sizes were nearly equivalent to comparable core configurations. That is, the BLC element produced drop sizes equivalent to a core element with an oxidizer post recess equal to 1 D_L while the scarfed post with swirl element produced drop sizes nearly equivalent to a nonscarfed core element.

Mixing experiments were conducted with the candidate peripheral elements to assess their mixing performance and potential chamber heat flux characteristics. Heat flux characteristics were evaluated by examination of wall zone mass and mixture ratio distributions.

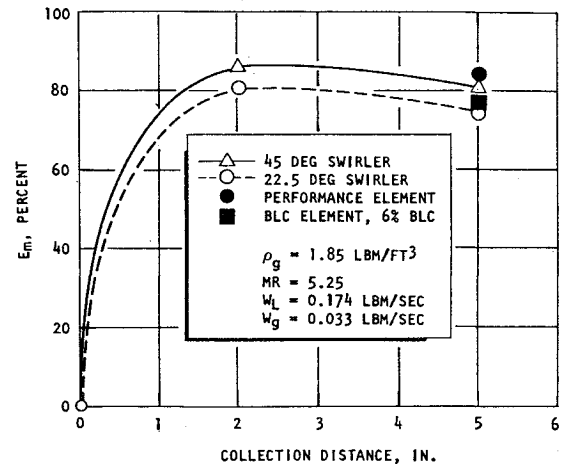

Fig. 3 Mixing performance of peripheral elements.

Mixing experiments were conducted with the BLC element to assess the effects of increasing the amount of BLC. As expected, increasing the amount of BLC flow resulted in lower ($\approx 2\%$) mixing levels. However, no significant qualitative differences were noted in the resulting mass and mixture ratio distributions.

The Rupe mixing performance, E_m, of the peripheral elements is presented in Fig. 3 as a function of distance from the injector. The mixing level at the injector face was assumed to be zero. Mixing levels for an equivalent core element configuration with zero oxidizer post recess and the BLC element are shown. At the 5-in. measurement plane, the mixing quality of the scarfed post with the 45° swirler was only slightly below that of the core element, but that of the element with a 22.5° swirler fell substantially lower.

Mass and mixture ratio distributions were examined by spacially plotting the "normalized" gas and liquid mass fluxes [$NMF_i = (w_i/A_i)_{\text{local}}/w_{i,\text{tot}}$, i = gas or liquid]. Note that the mass is normalized only with respect to total flowrate and not with respect to area. Plotting the normalized mass fluxes allows for a visual determination of the uniformity of the spray field. That is, if local values for the normalized liquid and gas flux coincide, then, at that point the local mixture ratio is equal to the injected mixture ratio. If the liquid values are higher than the gas, the local mixture ratio is greater than the injected mixture ratio, and vice versa.

Figure 4 presents "normalized" mass flux data for both the scarfed post and BLC configurations. Examination of the cold-flow data shows that both configurations possess characteristics which could provide enhanced injector/chamber compatibility. The flux profiles for the scarfed post with swirl

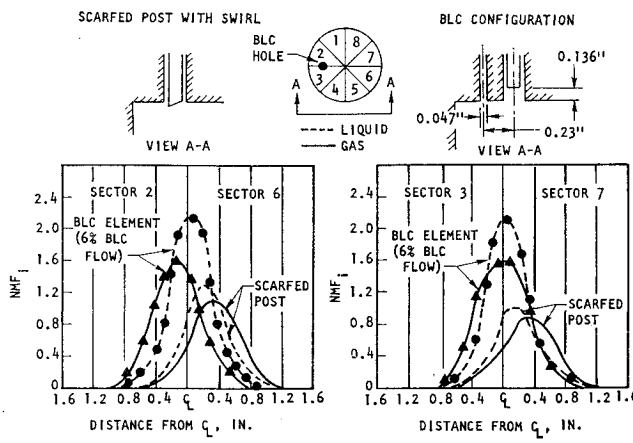

Fig. 4 Flux profiles of scarfed post and BLC elements.

show that the element displaces mass away from the wall region, but the local wall mixture ratios are higher than the injected mixture ratios. The flux profiles for the BLC tests show that liquid distribution is not affected by the showerhead BLC flow. However, the displacement of the gas distribution from the centerline of the element is evident. The resulting BLC element flowfield is characterized by a low wall region mixture ratio, but with relatively increased mass flux near the wall. The relative merits of each configuration as a peripheral element were investigated with single-element hot firings.

Core Element Hot-Fire Results

To select a core element for hot-fire evaluation, the cold-flow data were analyzed for predicted performance levels at both design and throttled conditions.[4] For this analysis, a baseline recess value of 1 D_L was selected. That value or postrecess had been used in similar FLOX/CH_4 programs with no postburning problems.[5]

In the analysis the wax drop sizes ($\bar{D}$) were corrected for the difference in physical properties between wax and FLOX using the empirical relations of Ingebo.[6] The resulting predicted FLOX drop size was utilized to predict $\eta_{c^*,vap}$ by employing a vaporization limited combustion model. The mixing limited c^* efficiency ($\eta_{c^*,mix}$) was obtained directly from the cold-flow mixing data. Based on the results of this analysis, a core element with $D_L = 0.136$ in., $D_g = 0.182$ in., was selected for hot-fire evaluation. The cold-flow studies indicated an optimum recess value of 1 D_L; however, postrecess was retained as a variable in the hot-fire series to determine at what value of postrecess would burning become established within the cup region.†

Parametric hot-fire experiments were conducted with the core element to assess the effects of oxidizer postrecess and to verify the predicted cold-flow mixing performance; chamber wall heat flux levels were also determined. Figure 5 presents performance (η_{c^*}) for FLOX postrecess values up to 2 D_L. The performance data were corrected for chamber heat loss based on measured heat flux data. The results of the hot-firing postrecess series are in essential agreement with the cold-flow data which indicated little change in element performance with increased postrecess depths.[4] Note that increasing the CH_4 temperature (i.e., increasing V_g) resulted in significantly higher performance. An increase in performance due to increased V_g was predicted by the cold-flow studies.[4]

A firing with $R = 3$ D_L was made. However, due to the failure of a pressure transducer, reliable motor performance data were not obtained. No injector hardware burning (neither oxidizer post nor injector face) was experienced.

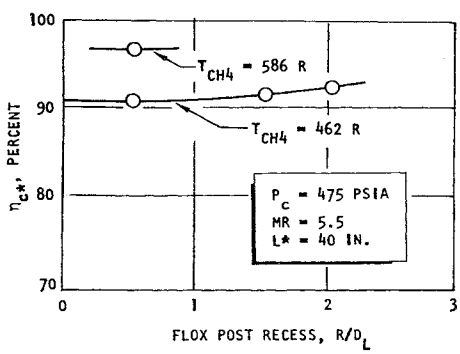

Fig. 5 Results of FLOX postrecess tests.

† The cup region of a recessed postelement is defined as the cylindrical region between the exit of the oxidizer post and the face of the injector.

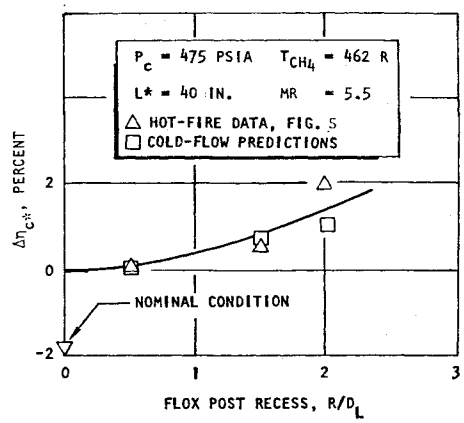

Fig. 6 Cold-flow/hot-fire correlations of postrecess tests.

Figure 6 presents a correlation of the cold-flow/hot-fire results in a manner which illustrates the ability of the cold-flow data to predict the parametric variation of the hot-fire results. The data are plotted as change in c^* efficiency ($\Delta\eta_{c^*}$) from the efficiency which was determined (in either hot-fire or cold-flow tests) from a nominal condition ($R = 0$, $L^* = 40$ in.) As indicated, the cold-flow data successfully predict the results of the hot-fire tests in that performance was not a strong function of postrecess.

The test series which was used to assess the performance effects of recessing the FLOX post at constant L^* (Fig. 5) provided information with regard to combustion effects within the cup region of the element. Figure 7 presents cup pressure drop for both hot-fire and cold-flow (i.e., nonburning) experiments. Plotting the parameter $\rho\Delta P$ allows comparison of the data which were conducted at slightly different gas-phase densities but at the same mass flowrate. A rapid divergence of cup pressure drop between hot-fire and cold-flow was found for postrecess values greater than 1-1/2 D_L. These data indicate that for postrecess depths greater than 1-1/2 D_L combustion occurred within the cup.

Figure 8 presents the results of the test series to verify the predicted cold-flow mixing level. Tests were conducted with $R = 0$ and chamber L^* was varied from 10 to 40 in. Extrapolation of the hot-fire data to values of $L^* > 40$ in., where

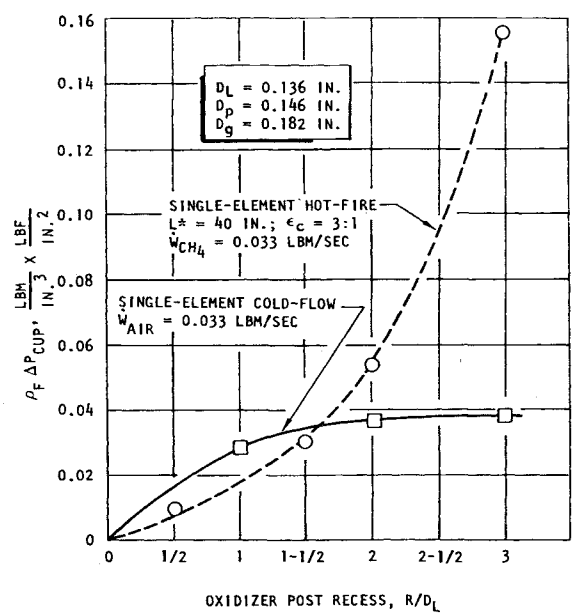

Fig. 7 Cup pressure drop.

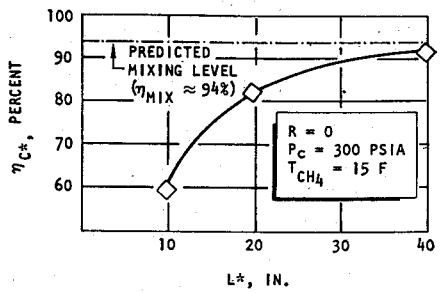

Fig. 8 Correlation of cold-flow/hot-fire mixing levels.

the performance loss due to vaporization would be insignificant, shows that the cold-flow and hot-fire mixing levels are essentially in agreement.

Figure 9 presents typical chamber wall heat flux profiles measured during the short duration ($\approx$3.5 sec) parametric hot-firing series. The data are for an oxidizer postrecess of 1/2 D_L for the 10-, 20-, and 40-in L^* chamber, respectively. No apparent dependency of chamber wall heat flux on postrecess was evident. Note that for all three chamber characteristic lengths, heat flux levels near the injector face are very low ($\approx$0.5 Btu/in.^{2}-sec). These data near the injector face were utilized to provide guidelines for the selection of a full-scale injector configuration in the later phases of the program.

Peripheral Element Hot-Fire Results

The two peripheral elements were hot-fired to determine their performance levels and chamber wall heat flux characteristics. Table 1 presents a comparison of the performance levels of the BLC and scarfed postperipheral element configurations ($T_{CH_4} \approx 470$°R). The recessed post ($R/D_L = 1$) with BLC performance was superior for all conditions tested.

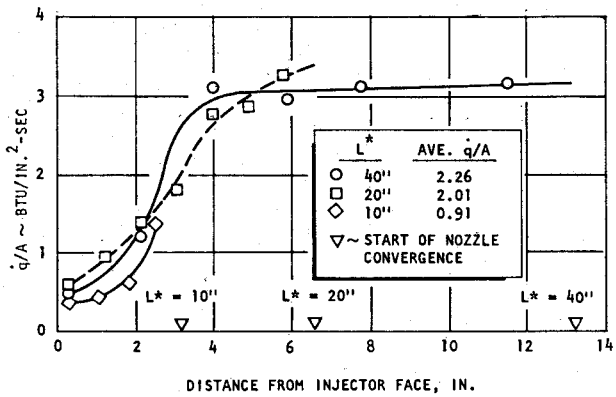

Fig. 9 Core element heat flux profiles.

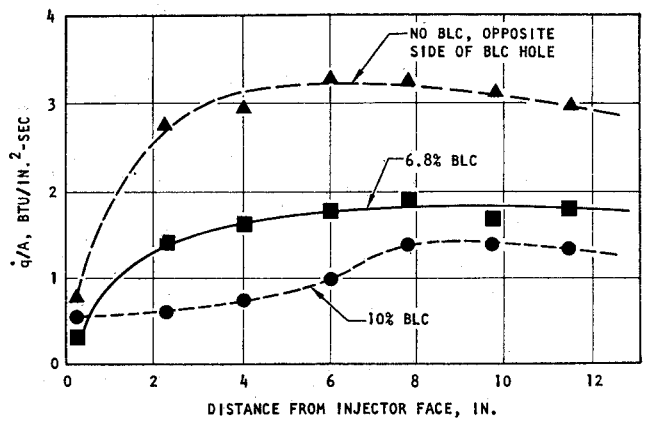

Fig. 10 BLC element heat flux profiles.

The single element graphite chambers ($L^* = 40$ in.) were instrumented with thermocouples to obtain axial heat flux data at two circumferential locations (180° apart) in the chamber. One row of thermocouples was oriented to be in line with the 0.047-in. BLC hole for that element type, and in the low mass flux region for the scarfed element type.

Figure 10 presents measured heat flux levels for tests conducted with BLC flow.‡ Shown in the plot are typical data for the chamber region which was 180° away from the BLC hole. Comparison of the heat flux levels along the two sides of the chamber provided a direct measure of the intended bias of heat flux away from one side of the element. As expected, significantly lower heat fluxes were measured in the BLC region.

Figure 11 presents chamber wall heat flux data for the scarfed post with swirl element at a mixture ratio of 5.28.

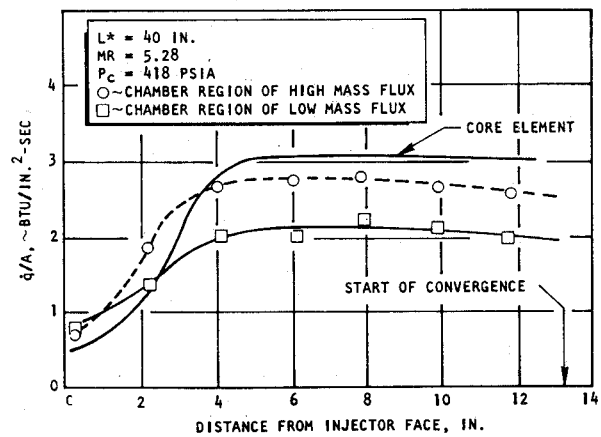

Fig. 11 Scarfed postheat flux profiles.

Table 1 Comparison of peripheral element hot-fire performance

Configuration	$MR_{overall}$, O/F	$MR_{element}$, O/F	P_c, psia	$\dot{w}_{BLC}$, lbm/sec	$\eta_{c^*,meas}$, %
Recessed post with 6.8% BLC, $R/D_L = 1$	4.86	6.03	441	0.0074	92.4
Recessed post with 10% BLC, $R/D_L = 1$	4.39	5·96	454	0.0110	93.8
Scarfed post with swirl	5.28	5.28	418	···	85.5
Scarfed post with swirl	3.02	3.02	454	···	72.2

‡ BLC percentage is defined as a percent of total fuel flow for a 3000 lbf FLOX/CH_4(g) engine at 500 psia assuming that $\frac{1}{3}$ of injector elements are located in the peripheral zone.

Also shown are heat flux data from a core element ($R = 1\ D_L$, $MR = 5.5$). As indicated, local heat flux levels in the low mass flux wall region were reduced approximately 30% from core element heat flux levels; whereas at the opposite side of the chamber heat fluxes correspond closely with those produced by the core element.

The results of the single-element hot-firing data can be physically interpreted in light of the mass flux profiles from the cold-flow experiments. The flux profiles for the scarfed post element (Fig. 4) show that the element displaces mass from the wall region, but the local wall mixture ratios are higher than the injected mixture ratios. The resulting characteristics of the BLC flowfield include a low wall region mixture ratio, but no reduction in mass flux. From the results of hot-firing experiments, it appears that the low mixture ratios produced by the BLC element were more effective in reducing wall heat fluxes than were the reduced wall mass flux generated by the scarfed post with swirl element. This result, in addition to the higher performance of the BLC configuration clearly makes that element a superior peripheral element.

Full-Scale Experimental Results

Injector Configuration

The design of the full-scale injector was unique in that it was based directly upon guidelines established from analysis of cold-flow and single-element hot-fire data. Heretofore, these data have not been available for the design of high-pressure space-storable rocket motors. The element configuration which was selected for the injector core was identical to the configuration which was utilized in the single-element hot-firing task with an oxidizer postrecess of 1-1/2 D_L (0.204 in.). Recessing the oxidizer posts to greater depths would have increased performance slightly (Fig. 5), but would have increased the possibility of oxidizer post burning (Fig. 7).

The peripheral zone element which was selected consisted of a recessed element with an adjacent showerhead BLC orifice. The BLC orifices were separately manifolded from the core methane manifold to permit variation of the amount of BLC. As in the single-element hot-fire studies, the BLC orifices were designed for an injection velocity equal to the fuel annulus velocity at the 6% BLC level ($\approx$350 fps).

For the 3000 lbf (sea level) injector, 43 elements were configured into a face pattern as shown schematically in Fig. 12. Note that the interelement spacing of the injector face pattern is relatively large ($\simeq$0.55 in. radially, $\simeq$0.50 in. circumferentially). The large interelement spacings were required with 70 lbf elements because the injector had to be compatible with an existing 3:1 contraction ratio chamber. Use of a lower contraction ratio chamber with a coaxial injector appears feasible.

The chamber wall heat flux measurements made during the single-element hot-fire series indicated very low heat fluxes near the injector face (Figs. 9–11). Based on these data, an analysis of the temperature distribution in the injector face indicated that cooling of the face would not be required. Prior to this program, high-pressure FLOX/CH_4(g) programs had employed some method of injector face cooling (i.e., Regimesh etc.).[7] Elimination of the injector face cooling requirements significantly reduced the complexity and fabrication cost of the full-scale injector.

Cold-Flow Results

Cold-flow mixing tests with the full-scale injector were performed in a pressurized gas/liquid mixing facility.[4] In these tests, a pressurized chamber was employed which was equal in diameter to the hot-fire chamber (3.880 in.). All

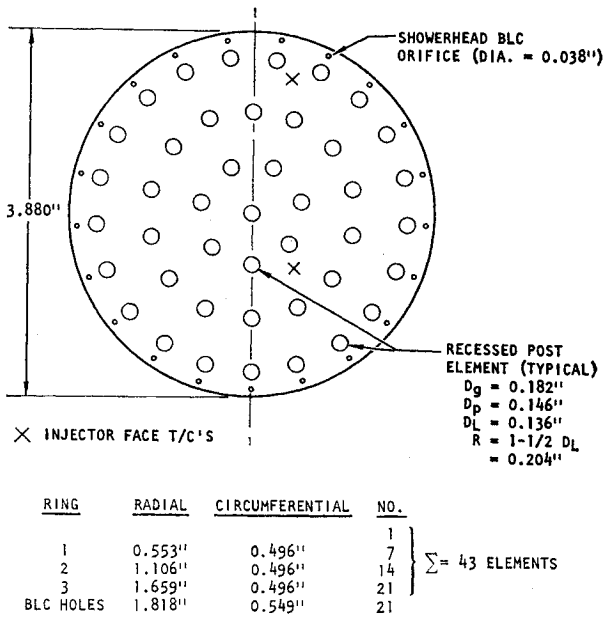

RING	RADIAL	CIRCUMFERENTIAL	NO.	
			1	
1	0.553"	0.496"	7	
2	1.106"	0.496"	14	∑= 43 ELEMENTS
3	1.659"	0.496"	21	
BLC HOLES	1.818"	0.549"	21	

Fig. 12 Face pattern of full-scale injector.

measurements were made 5 in. from the injector face as in the single-element mixing experiments. These tests were conducted to determine effects upon mixing of over-all injected mixture ratio, pressure throttling, and percentage of BLC flowrate. Figure 13 presents full-scale cold-flow results, and results of analogous tests which were conducted with single-element models.

The top portion of Fig. 13 presents results for experiments with no BLC flow. The predicted mixing performance was approximately 98% at the simulated design condition. Since single-element and full-scale mixing efficiencies were almost

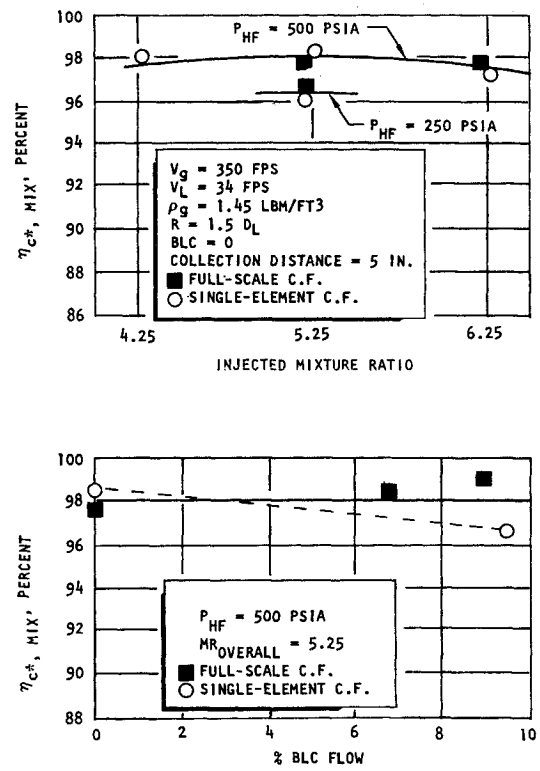

Fig. 13 Results of full-scale mixing tests.

identical, the data suggest that interelement mixing effects are of second order for this particular injector configuration. These results are not too surprising when the low element density of the injector is considered.

The lower portion of Fig. 13 shows the results of the tests with BLC flow (6.8 and 9%). The predicted single-element line (dashed) was derived by mass weighting (based on percent of peripheral mass flow) the results from experiments conducted with a single-element core and a BLC type element. As indicated, the single-element and full-scale mixing data predict little change in mixing-limited performance with increased BLC flowrate. The results of the single-element hot-fire series (Table 1) showed that increasing BLC flow had little effect on over-all performance.

Hot-Fire Results

Full-scale, hot-fire tests were conducted with parametric variations of injected mixture ratio, chamber pressure, and percentage of BLC flow. Appropriate correction factors (chamber heat loss, nozzle divergence losses, etc.) were applied to the measured data.[4]

Figures 14 and 15 present the results of the test series to determine the effects of injected mixture ratio, throttling, and percent BLC flow. The heat loss correction factors were based upon measured chamber heat flux levels determined during the short duration ($\simeq$3 sec) tests. Because of low chamber heat flux levels, the c^* correction was not large, amounting to approximately 0.7% at the design point. The data shown in Fig. 14 for the 44-sec duration test were not corrected for chamber heat loss because calculations showed that for run times greater than 10 sec the chamber operated nearly adiabatically. At the design point ($P_c = 500$ psia, $MR = 5.25$), corrected c^* performance was 98.8%. Throttling of the injector resulted in a moderate reduction in η_{c^*}, but to values no lower than approximately 95%.

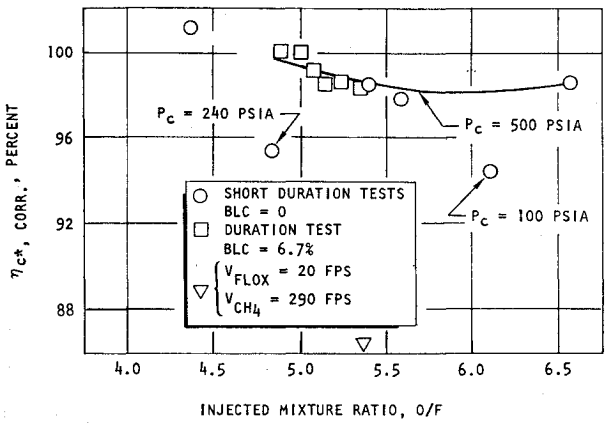

Fig. 14 Hot-fire performance data.

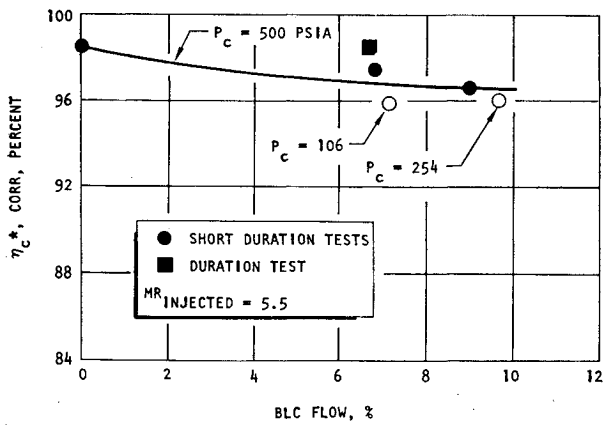

Fig. 15 Hot-fire performance data with BLC flow.

It should be noted that injected methane temperatures were low ($\approx$2 to 15°F), which resulted in high injected gas densities ($\rho_g \approx 1.8$ lbm/ft) and low methane gas gap velocities ($\approx$290 fps). It was previously demonstrated that supplying the methane at higher temperatures ($\approx$120°F) resulted in substantial increases in performance (Fig. 5). If the methane were supplied at simulated regenerative chamber temperatures ($\approx$800°F), it is estimated that injector performance would be near 100% for the range of parameters investigated.

Figure 15 presents the effects of BLC flow (as % of total CH_4 flow) on injector performance. A nominal BLC flow of 6.0% resulted in approximately a 1% loss performance. Note that performance was nearly constant over a 5:1 throttling range when BLC was employed. In addition, available instrumentation revealed no instabilities (neither high frequency or chugging) as the engine was throttled. This excellent stability was noted both with and without BLC flow.

Chamber heat flux data were obtained during the short-duration parametric tests by placing small thermocouples in selected locations within the ATJ graphite chamber. Chamber wall heat flux values were then calculated by assuming that the chamber wall was a semi-infinite slab suddenly exposed to constant $\dot{q}/A$. Figure 16 presents typical injector face and chamber heat flux profiles which show the effect of BLC flow. The data were reduced at a time during the run ($\approx$2.7 sec in a 3-sec test) where the chamber wall temperature was calculated (based on measured inner wall temperatures) to be approximately 1000°F. Thus, the data are comparable with regeneratively cooled chamber data with wall temperatures on the order of 1000°F. As expected, the BLC flow was found to be most effective near the injector end of the chamber.

An injector stability rating test was conducted at a nominal operating point ($P_c = 500$ psia, $MR = 5.25$, BLC = 6.7%, $L^* = 40$ in.) by sequentially bombing the engine with bombs of increasing size. Available Photocon data (FLOX and CH_4 manifold pressures) revealed a maximum overpressure of approximately 1100 psi. No injector damage of any kind was sustained during the bomb test. Recovery to normal chamber pressure was achieved in approximately 15 msec.[4]

A 44-sec duration test was conducted using a nominal BLC flow of 6.7% in the 40-in. L^* chamber. Figure 14 presents measured c^* performance based on thrust for the duration test. For this test, pressure taps and thermocouples were not placed in the graphite-lined chamber. Measured throat area change during the run was only 0.75%. The injector face thermocouples revealed an extremely low face temperature ($\approx$50°F steady state) during the duration test.[4] Clearly, for this program, injector face cooling (i.e., Regimesh,

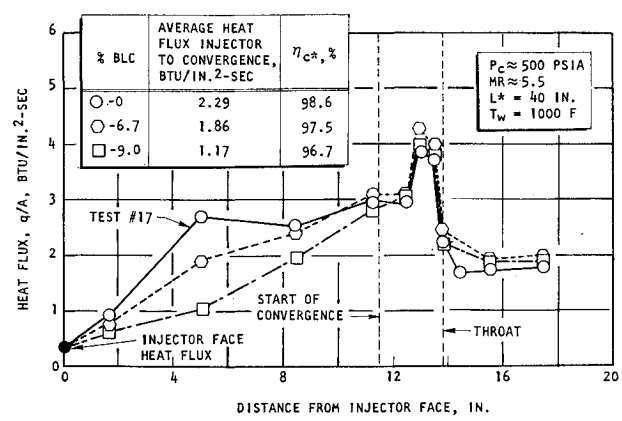

Fig. 16 Chamber heat flux profiles.

etc.) would have been a needless expense. This illustrates the value of subscale (single-element) experiments which showed a priori that injector face cooling was not required.

Dissusion of Results

Full-Scale Cold-Flow/Hot-Fire Correlation

The full-scale cold-flow mixing data of Fig. 13 and the single-element atomization data were analyzed to determine the degree of correlation between cold-flow performance predictions and hot-fire results. As in the single-element cold-flow/hot-fire correlation, the over-all engine performance was assumed to be the product of a mixing-limited η_{c^*} and a vaporization-limited η_{c^*} efficiency.

Figure 17 presents the results of the correlation analysis of the cold-flow/hot-fire results for the full-scale injector. The data are plotted in a manner which illustrates the ability of the cold-flow data to predict the parametric variations of the hot-firing series (i.e., chamber pressure, injected mixture ratio, and % BLC flow). The dependent parameter in the three graphs shown in Fig. 17 is the relative change in η_{c^*} ($\Delta\eta_{c^*}$) from the efficiency which was determined (in either hot-fire or cold-flow tests) at the nominal design condition ($P_c = 500$ psia, $MR = 5.25$, and BLC = 0). As indicated, the cold-flow data successfully predicted reduced performance levels when: 1) the engine was throttled, 2) the over-all injected ratio was increased, and 3) the percentage of the BLC flow was increased.

To determine if the cold-flow data could predict the absolute performance level of the full-scale injector, the hot-fire test data were analyzed for all conditions at which full-scale mixing tests were performed. Table 2 summarizes the pertinent data employed in the analysis. The average deviation of the five hot-fire tests from the performance levels predicted by cold-flow was 2.2%.

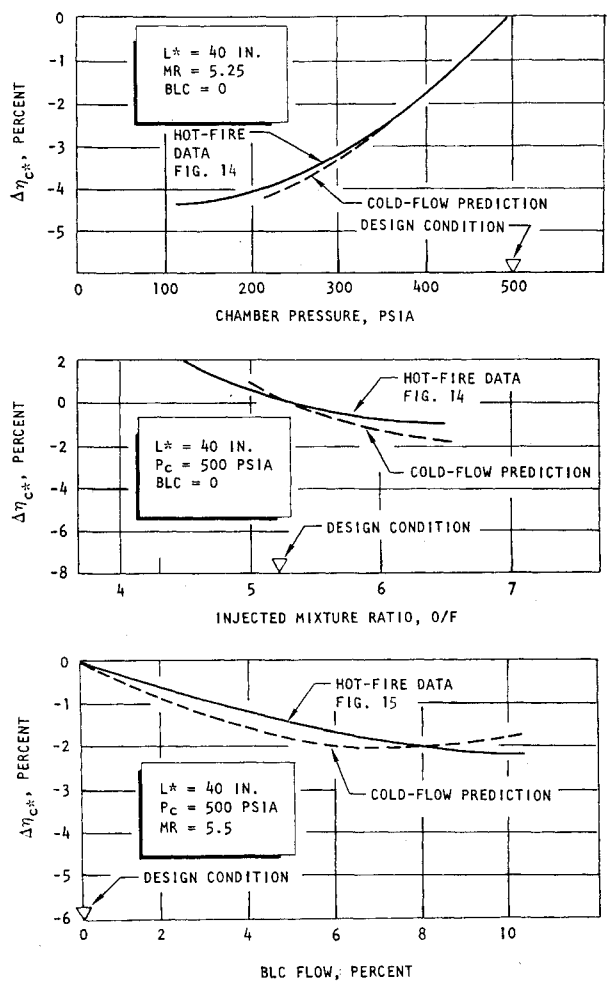

Fig. 17 Full-scale cold-flow/hot-fire correlation.

Performance/Chamber Compatibility Characteristics

The full-scale injector of this study met the performance and chamber compatibility goals of the program. Injector performance was 99% of the theroetical shifting characteristic velocity at the design point. Acceptable injector/thrust chamber compatibility was demonstrated both in the short-duration parametric tests and in the 44-sec duration firing. Injector face temperature data from the duration firing indicated that the injector should be operable for an indefinite period of time.

From the results of this program, certain single-element hot-fire data suggest direct applicability to full-scale injector design. As a specific example, chamber wall heat flux data measured in single-element chambers (Fig. 14) suggested that cooling of the full-scale injector face would not be required. Based on these data, the full-scale injector face was not cooled and the test results verified that cooling was not required. Figure 18 presents a correlation between single-

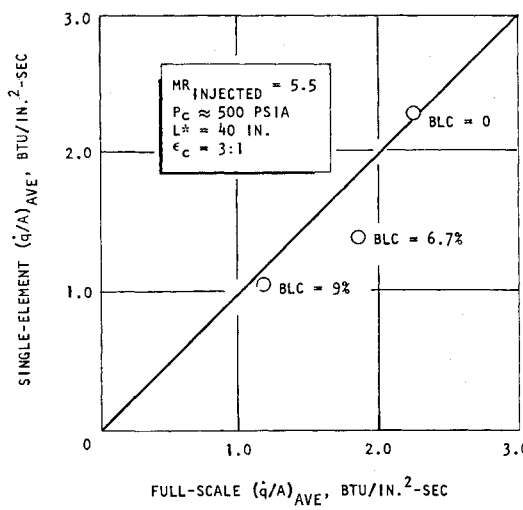

Fig. 18 Correlation of average chamber wall heat flux.

Table 2 Full-scale performance correlation

Hot-fire test no.	P_c, psia	MR, O/F	BLC, %	$\bar{D}_{wax}$, μ	$\bar{D}_{FLOX}$, μ	Cold-flow $\eta_{c^*,vap}$, %	Cold-flow $\eta_{c^*,mix}$, %	Cold-flow η_{c^*}, %	Hot-fire η_{c^*}, %
17	512	5.38	0	600	236	98.0	97.7	95.7	98.4
19	518	6.56	0	720	284	96.0	97.7	93.8	98.3
20	242	4.84	0	640	252	97.5	96.6	94.2	95.3
22	516	5.77	6.7	690	271	96.7	98.6	95.4	97.5
23	507	5.53	9.0	680	258	97.1	99.0	96.2	96.7

element and full-scale chamber heat flux levels (injector to start of convergence) which suggest the use of low-cost, single-element or subscale hardware to determine injector/chamber compatibility characteristics.

Pressure throttling of the injector was not a requirement of the program; however, throttling tests resulted in stable operation at high performance levels ($\approx 94.5\%$) over a 5:1 throttling range. In the deeply throttled mode ($P_c = 100$ psia) the injector exhibited neither low- (chugging) nor high-frequency instabilities. This is especially noteworthy because at this operating condition total injector pressure drop was approximately 18 psi.

Summary

An experimental program has been conducted which utilized single-element, cold-flow/hot-fire experiments to establish design criteria for a high performance gas/liquid ($FLOX/CH_4$) coaxial injector. The approach and techniques employed resulted in the direct design of an injector which met or exceeded performance and chamber compatibility goals without any need for the traditional "cut-and-try" injector development methods. These same design techniques can be applied to other high-performance injector systems to reduce both the time and cost necessary to arrive at an optimum injector configuration.

References

[1] Falk, A. Y. et al., "Space Storable Propellant Performance Study," NASA CR-72487 Nov. 1968, Rocketdyne Div./Rockwell International, Canoga Park, Calif.

[2] "Correlation of Spray Parameters with Rocket Engine Performance," AFRPL-TR-68-147, Contract FO4611-67-C-0081, June 1968, Rocketdyne Div./Rockwell International, Canoga Park, Calif.

[3] Burick, R. J., "Atomization and Mixing Characteristics of Gas/Liquid Coaxial Injector Elements," *Journal of Spacecraft and Rockets*, Vol. 9, No. 5, May 1972, pp. 326–331.

[4] Burick, R. J., "Space Storable Propellant Performance Program-Coaxial Injector Characterization," NASA CR-120936, April 1972, Rocketdyne Div./Rockwell International, Canoga Park, Calif.

[5] Pauckert, R. P., "Space Storable Regenerative Cooling Investigation," NASA CR-72705, June 1970, Rocketdyne Div./Rockwell International, Canoga Park, Calif.

[6] Ingebo, R. D. et al., "Dropsize Distribution for Crosscurrent Breakup of Liquid Jets in Airstreams," TN-4087, 1957, NASA.

[7] "Space Storable Regenerative Cooling Investigation," NASA CR-72704, Oct. 1971, Pratt and Whitney Aircraft, Florida Research and Development Center, West Palm Beach, Fla.

[8] Mehegan, P. F. et. al., "Investigation of Gas-Augmented Injectors," NASA CR-72720, Sept. 1970, Rocketdyne Div./Rockwell International, Canoga Park, Calif.